

Cite this article as: Wang Xuezheng, Song Xiaolei, Duan Zhenxin, et al. High Temperature Mechanical Properties and Deformation Mechanism of Equiaxed Fine-Grained Ti-45Al-7Nb Alloys[J]. Rare Metal Materials and Engineering, 2022, 51(05): 1543-1549.

ARTICLE

High Temperature Mechanical Properties and Deformation Mechanism of Equiaxed Fine-Grained Ti-45Al-7Nb Alloys

Wang Xuezheng, Song Xiaolei, Duan Zhenxin, Chen Hua

Changchun University of Technology, Changchun 130012, China

Abstract: The duplex Ti-45Al-7Nb (at%) alloys with equiaxed fine grains were prepared by powder metallurgy method. The high temperature mechanical properties of the alloys at 900, 950, and 1000 °C under the strain rates of 1×10^{-3} , 1×10^{-4} , and $5 \times 10^{-5} \text{ s}^{-1}$ were investigated, and the corresponding deformation mechanism was also discussed. Results show that the tensile strength is decreased whereas the elongation is greatly increased at elevated temperatures or under decrescent strain rates. Since the small grains are easy to achieve deformation and coordination, the elongation of the small grain alloys is significantly higher than that of coarse grain alloys. The alloys form a large number of voids at the fractures after high temperature tension. Long cracks perpendicular to the tensile direction are formed at the front fracture. Besides, the grain boundary sliding, grain twinning, and dynamic recrystallization also lead to the deformation of alloys, thus improving the microstructure ductility.

Key words: duplex TiAl alloy; equiaxed fine grain; high temperature tension; deformation mechanism

TiAl alloy has the characteristics of high specific strength, high specific elastic modulus, high temperature creep resistance, and excellent oxidation resistance, thereby showing great potential in the new generation aerospace and automotive fields^[1-5]. However, the inferior hot working property of TiAl alloy causes difficulties in working at high temperatures, and cracks and fractures are easily generated under increased surface tensile stress^[6], which all restrict its application. Therefore, it is necessary to enhance the plasticity of TiAl alloys. In recent years, the fine-grain strengthening method is widely used to improve the mechanical properties of TiAl alloys^[7-10], since the refined grains are conducive to grain boundary sliding and grain diffusion for good plastic behavior of the alloys^[11].

At present, there are many preparation methods for TiAl alloys, including the powder metallurgy, forging, and casting. However, the ingot structure may produce defects during the casting process, such as composition segregation, shrinkage cavity, and difference in grain size. Millett et al^[12] prepared the Ti-52Al as-cast alloy consisting of large grains and many dendritic grains, whose high-temperature mechanical properties were significantly reduced. Zhu et al^[13] prepared Ti-

20Al-22Nb (at%) alloy by casting method. Due to the non-equilibrium solidification, the uneven structure appears and the loose defects in structure occur, resulting in low plasticity of alloys. In contrast, TiAl alloys prepared by powder metallurgy method show the fine-grained structure. Salishchev et al^[11] prepared the TiAl alloy by powder metallurgy method, which had TiAl and Ti₃Al intermetallic compounds with uniform and fine equiaxed structures. Liu et al^[14] obtained the TiAl-based alloy by the mechanical alloying method. Yu et al^[15] conducted the high-temperature tensile test at 850 °C on the fine-grained Ti-45Al-2Cr-2Nb-1B alloys, and found that the TiAl alloy has the excellent tensile property, and its elongation is 63%~101%. Therefore, the powder metallurgy method has the advantages of simple operation, low cost, and good formability, which is suitable to prepare TiAl alloys^[16].

In addition, TiAl alloys are required to work in complex high-temperature environments^[17], so the high Nb-containing TiAl alloys have been developed^[18,19]. Ref.[20] shows that the Nb addition can improve the high-temperature strength and ductility of TiAl alloy. Kothari et al^[21] found that Nb can decrease the stacking fault energy of TiAl alloys, and the

Received date: May 18, 2021

Foundation item: National Natural Science Foundation of China (51371038)

Corresponding author: Chen Hua, Ph. D., Professor, College of Materials Science and Engineering, Changchun University of Technology, Changchun 130012, P. R. China, Tel: 0086-431-85716396, E-mail: chenhua@ccut.edu.cn

Copyright © 2022, Northwest Institute for Nonferrous Metal Research. Published by Science Press. All rights reserved.

movement of some dislocations is promoted, which improves the plasticity of TiAl alloys. Du et al^[22] prepared Ti-45Al-8Nb alloy and found that the elongation of TiAl alloy is 237% at 1050 °C. The TiAl-Nb alloys show great potential in the test of automobile exhaust valves^[23]. However, the TiAl-Nb alloy prepared by powder metallurgy method is rarely investigated^[24,25].

In this study, the equiaxed fine-grained Ti-45Al-7Nb alloy was prepared by powder metallurgy. The tensile properties of the alloy at different elevated temperatures and strain rates were investigated. The characteristics of stress and the mechanism of microstructure evolution during the deformation process were also analyzed.

1 Experiment

Ti, Al, and Nb powders were mixed by high-energy mechanical ball milling, whose average particle size was 12, 14, and 9 μm, respectively. The purity of the three powders was higher than 99.9%. The GCr15 steel ball milling tanks and grinding balls were used in the high-energy ball milling. The diameter of the grinding balls was 10 and 15 mm, the number ratio of large and small grinding balls was 1:2, and the mass ratio of balls to powders was 10:1. The powders were mixed at 150 r/min for 30 min, and then rotated in the high-energy ball milling at a rotation speed of 550 r/min for 40 h to obtain the mechanically alloyed powders. In order to prevent the oxidation of titanium and other powders, the mixed powders were prepared under the argon atmosphere. The vacuum hot pressing sintering process was conducted at 1200 °C under the pressure of 30 MPa for 1 h.

The tensile specimens with the dimension of 2 mm×2 mm×10 mm were cut from the alloy. The tensile tests were conducted on a WDW-200 electronic universal testing machine at room temperature, 900, 950, and 1000 °C, separately. The tensile strain rates were 1×10^{-3} , 1×10^{-4} , and 5×10^{-5} s⁻¹. Fig.1 shows the schematic diagram of preparation and experiment processes. Before the high temperature tensile tests, all specimens were heated at the test temperature for 5 min to study microstructure evolution during the experiment.

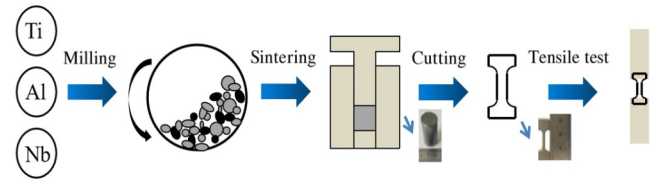


Fig.1 Schematic diagram of preparation and experiment processes of Ti-45Al-7Nb alloys

Once the specimens fractured, they were immediately quenched in water to maintain the high-temperature structures.

The phase components of the mixed powders and sintered specimens were examined by X-ray diffraction (XRD). The microstructures before and after tensile tests and fracture surfaces were observed by scanning electron microscope (SEM). The software ImageJ was used to count the grains in microstructure. The field emission transmission electron microscope (TEM) was used to analyze the structural characteristics of the alloys.

2 Results and Discussion

2.1 Sintered microstructure

Fig. 2a and 2b show XRD patterns of the mechanically alloyed powders and the sintered Ti-45Al-7Nb alloys, respectively. Fig. 2c shows TEM morphology and selected area electron diffraction (SAED) patterns of the sintered Ti-45Al-7Nb alloys. TiAl and Ti₃Al phases appear in the powders after ball milling. The collisions between the powders generate energy for atomic diffusion and solid-phase reaction during the high-energy ball milling and long-time ball milling. Mechanical alloying occurs in the powders, and thereby a compound phase forms. The sintered duplex Ti-45Al-7Nb alloy is also composed of TiAl and Ti₃Al phases, but its XRD pattern is obviously different. The intensity of diffraction peaks of the sintered specimen is greatly increased, because the specimen density is increased after hot pressing sintering at high temperature. The occurrence of lattice distortion in the alloy causes different crystal surfaces. Thus, the new

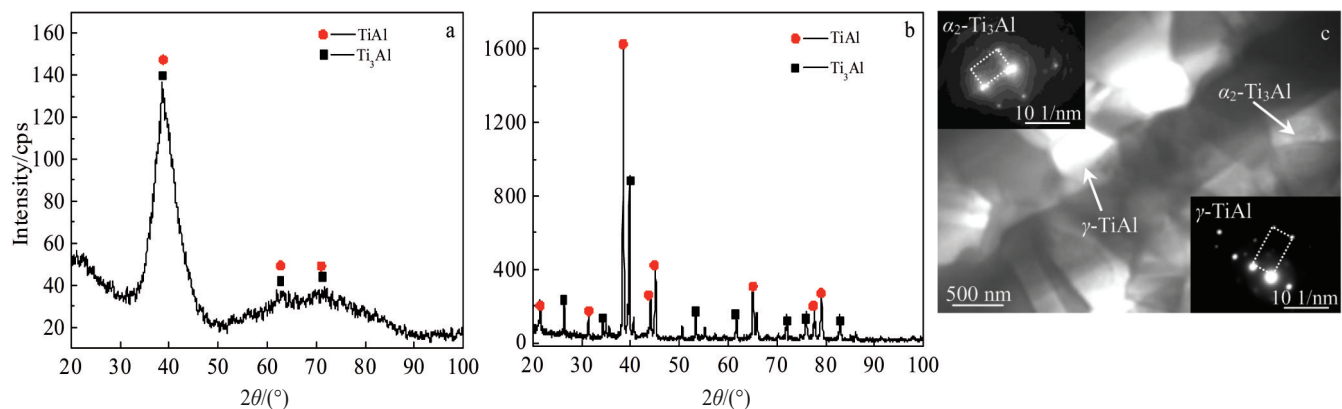


Fig.2 XRD patterns of mixed powder (a) and sintered Ti-45Al-7Nb alloy (b); TEM morphology and SAED patterns of sintered Ti-45Al-7Nb alloy (c)

diffraction peaks appear. Meanwhile, the γ -TiAl phase and the α_2 -Ti₃Al phase can also be observed.

The equiaxed and uniform microstructure of the sintered Ti-45Al-7Nb alloy is shown in Fig. 3a. The microstructure is composed of γ -TiAl matrix phase and α_2 -Ti₃Al phase. The average grain size of TiAl and Ti₃Al is about 1.11 and 0.75 μm , respectively. Liu et al.^[26] also used powder metallurgy to prepare Ti-45Al-7Nb-0.3W alloy, but that alloy showed the layered structure and the grain size was only about 20 μm .

2.2 Tensile properties and fracture characteristics

Fig.4 shows the tensile true stress-true strain curves of Ti-45Al-7Nb alloys at different temperatures and different strain rates. As shown in Fig.4a, the tensile strength of the alloy is 649 MPa and the elongation is only 3.3% at room temperature at the strain rate of $1 \times 10^{-4} \text{ s}^{-1}$, because the intrinsic brittleness of γ -TiAl-based alloys leads to low room temperature plasticity and low ductility. At the same strain rate of $1 \times 10^{-4} \text{ s}^{-1}$, when the temperature is 900 °C, the tensile strength decreases to 126 MPa and the elongation reaches 65%. With further increasing the temperature to 1000 °C, the tensile strength declines to 17.2 MPa, while the elongation is increased to 175%. The equiaxed γ -TiAl-based alloy has obvious elongation fracture characteristics. As the temperature rises, the elongation exhibits monotonous character. During the tensile process, the dislocation nucleation occurs at the trifurcate grain boundaries to deform the alloy. But the grain boundaries hinder the dislocation glide. The obvious grain rotation and grain boundary sliding occur in the alloy with increasing the temperature, which easily causes the dislocation glide^[27-29]. Thus, the tensile strength of the alloy decreases, the toughness increases, and the elongation

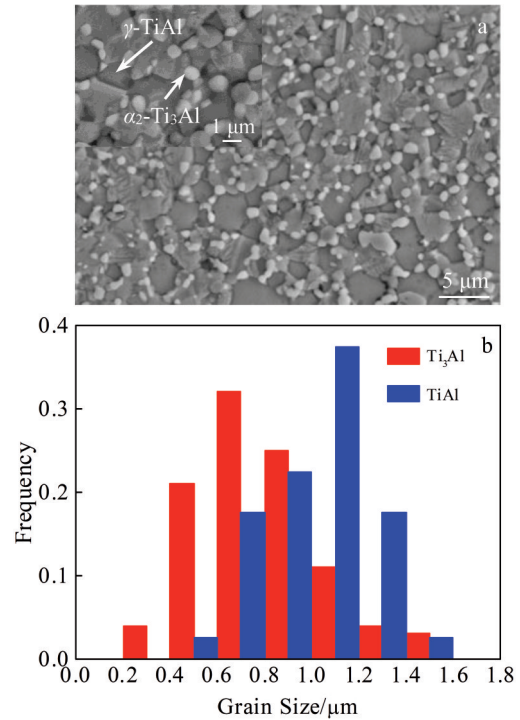


Fig.3 SEM microstructure (a) and grain size distribution (b) of sintered Ti-45Al-7Nb alloy

gradually increases.

As shown in Fig. 4b, at 900 °C, the tensile strength is decreased from 246 MPa to 102 MPa with decreasing the strain rate from $1 \times 10^{-3} \text{ s}^{-1}$ to $5 \times 10^{-5} \text{ s}^{-1}$, while the elongation is increased from 4.4% to 84.9%. Under high strain rates, the

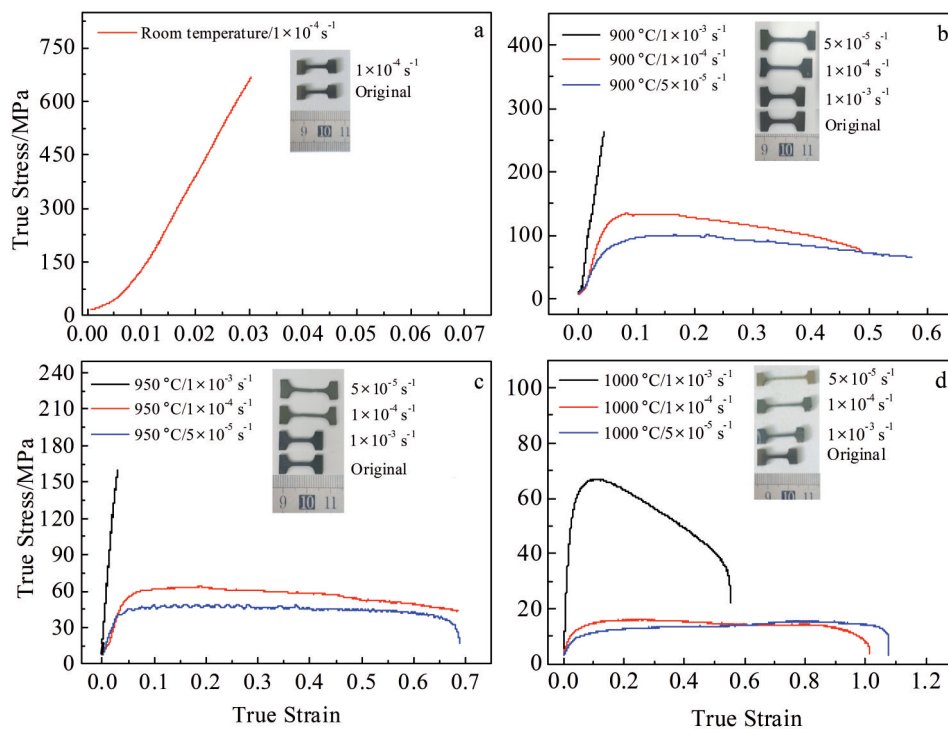


Fig.4 True stress-true strain curves of Ti-45Al-7Nb alloys at different temperatures and strain rates

dislocation density increases rapidly at the beginning of the tensile test. The defect formation speed is faster than the recovery speed, and the dislocation glide cannot proceed, resulting in a rapid increase in stress. Besides, the high strain rate also leads to the fact that dynamic recovery and recrystallization growth cannot proceed in time during plastic deformation, which easily generates microcracks in the alloy and reduces the elongation. As the strain rate decreases, the dislocation density is decreased. The dynamic recovery occurs to reduce the dislocation plugging, leading to a significant reduction in lattice distortion, dislocation glide, and diffusion in the alloy. Thus, the tensile strength reduces, whereas the elongation significantly increases.

Under different temperatures, all true stress-true strain curves show similar rules: the stress begins to increase sharply until the ultimate tensile strength is reached. Then the stress is gradually decreased with increasing the strain. Moreover, the steady state of the tensile curve becomes longer and the ultimate tensile strength is lower with increasing the temperature, which is also a typical feature of many metal materials. Compared with other TiAl alloys^[27,30,31], the tensile strength of the alloy with equiaxed fine structure prepared by powder metallurgy is significantly lower, as listed in Table 1. This is because the fine grains cause the grain boundary glide coordination, which is conducive to grain boundary movement and crystal grain rotation. Thus, the stress is reduced and the alloy is softened.

Fig. 5 shows the fracture surfaces of Ti-45Al-7Nb alloys after tensile tests at 900 °C. It can be seen that there are apparent cleavage steps and cleavage fractures in the

specimen at the strain rate of $1 \times 10^{-3} \text{ s}^{-1}$, proving that the plastic deformation does not occur at low temperature and high strain rate. As the strain rate decreases to 1×10^{-4} and $5 \times 10^{-5} \text{ s}^{-1}$, the voids can be clearly observed in Fig. 5b and 5c, respectively. The size and the number of voids are gradually increased with decreasing the strain rate, leading to more severe plastic deformation. Therefore, the appearance of voids increases the ductility and elongation of alloys. During the high-temperature tensile tests, the strain rate has a great influence on the deformation of specimens, because the decreased strain rate can activate the source of dislocations and promote the dislocation glide, thereby promoting the plastic deformation.

2.3 Deformation mechanism

Fig. 6 shows the microstructure near the fracture of the tensile specimen at different temperatures and strain rates. The specimen undergoes cleavage fracture, and there are microcracks near the fracture under the condition of strain rate of $1 \times 10^{-3} \text{ s}^{-1}$ and temperature of 900 °C. This is because the cracks are not completely propagated due to the premature fracture. As the temperature rises to 1000 °C, the cleavage fracture changes to ductile fracture. The microcracks have sufficient time to grow into long strip cracks, as shown in Fig. 6b. At the same temperature, when the strain rate decreases to $5 \times 10^{-5} \text{ s}^{-1}$, a large number of long strip cracks are formed in the front of the specimen fracture region (Fig. 6c).

The expansion direction of most cracks is perpendicular to the tensile direction, which is mainly caused by the tensile stress at the grain boundary. The stress is quickly concentrated

Table 1 Mechanical properties of TiAl-based alloys

Alloy	Grain size/ μm	Tensile temperature/ $^{\circ}\text{C}$	Strain rate/ s^{-1}	Strength/MPa	Elongation/%	Ref.	
Ti-45Al-7Nb-0.3W (lamellar)	8	950	1×10^{-3}	307	-	[30]	
Ti-46Al-9Nb (lamellar)	5	Room temperature	1×10^{-4}	881	2.5	[27]	
		1000	5×10^{-4}	85	93		
Ti-45.2Al-3.5(Nb,Gr,B) (lamellar)	3	1000	1×10^{-3}	140	-	[31]	
		Room temperature	1×10^{-4}	649	3.3		
		950	1×10^{-3}	159	7.45		
Ti-45Al-7Nb (equiaxed)	0.75~1		1×10^{-3}	67.1	74	-	
			1000	1×10^{-4}	17.2		175
			5×10^{-5}	15.5	194		

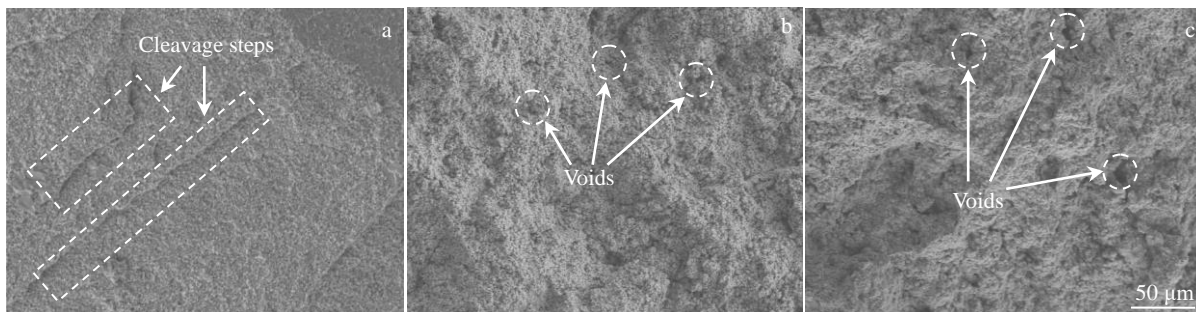


Fig.5 SEM images of tensile fracture surface at 900 °C and different strain rates: (a) $1 \times 10^{-3} \text{ s}^{-1}$, (b) $1 \times 10^{-4} \text{ s}^{-1}$, and (c) $5 \times 10^{-5} \text{ s}^{-1}$

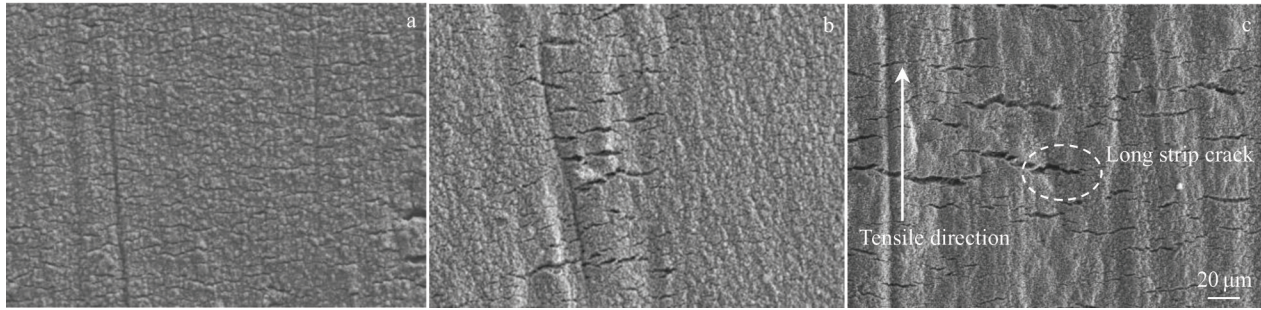


Fig.6 SEM images of Ti-45Al-7Nb alloys near tensile fracture region under different conditions: (a) 900 °C/1×10⁻³ s⁻¹; (b) 1000 °C/1×10⁻³ s⁻¹; (c) 1000 °C/5×10⁻⁵ s⁻¹

when the tensile force of specimens reaches the critical stress value, which causes necking in the local area of specimens. Moreover, the stress state of the specimen changes from one-way to three-way. Therefore, the plastic deformation hardly proceeds, and the second phase in the center of specimen is separated from the matrix to form small cavities, which continue to grow and integrate into cracks, eventually leading to the fracture, as shown in Fig.7. This phenomenon is similar to the fracture structure of most TiAl alloys after plastic deformation. However, the evolution of the crack structures and the nucleation of the cracks during the tensile process both enhance the tensile properties. Besides, the Ti-45Al-7Nb alloy obtains the maximum elongation of 194% under the condition of 1000 °C and 5×10⁻⁵ s⁻¹.

Fig.8 shows TEM images of dislocation and twinning in Ti-45Al-7Nb alloy after tensile test at 1000 °C under strain rate of 5×10⁻⁵ s⁻¹. A high density of dislocations can be observed near the grain boundary of γ phase, and the twins are formed in γ grains. The formed twins divide the γ/γ grains. The twin stripes formed at the γ/γ interface are clear and distinct. When the tensile specimen undergoes plastic deformation at 1000 °C under strain rate of 5×10⁻⁵ s⁻¹, the α_2 phase in the equiaxed ultrafine-grained γ -TiAl alloy has a hindering effect on the dislocations. Compared with the specimen before tensile test (Fig.2c), it can be seen that the sub-crystal dislocations at the grain boundaries are increased with the entanglement and accumulation of dislocations after tensile test. The sub-grains grow with the migration of grain boundaries, and the recrystallization occurs at some sub-grains to refine the grains, thereby promoting the grain boundary glide. During the

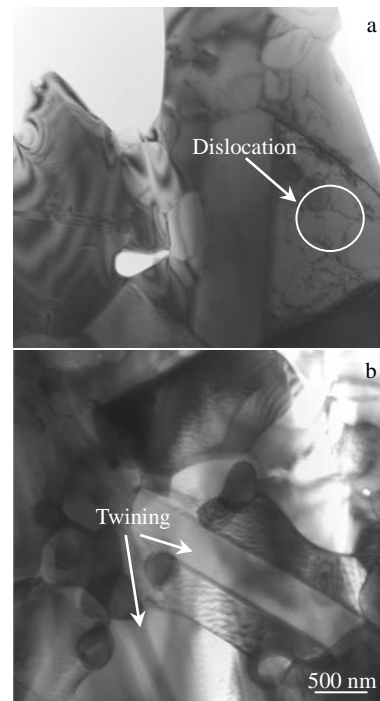


Fig.8 TEM images of dislocation (a) and twinning (b) in Ti-45Al-7Nb alloy after tensile test at 1000 °C and strain rate of 5×10⁻⁵ s⁻¹

tensile process, the grain boundary glide causes the stress concentration near the glide region. The dislocation movement releases the deformation stress to promote the grain boundary glide. Thus, a large number of dislocations are formed (Fig.8a).

In the initial stage of plastic deformation, the increase in dislocations and the interaction between dislocations leads to rapid increase in stress. After reaching the critical strain, the diffusion of atoms, the cross slip of dislocations, and the migration of grain boundaries are improved, which is conducive to dynamic recrystallization (DRX) nucleation and crystal nucleation growth. Fig. 9 shows a large number of recrystallized grains with grain size of about 250 nm. Because the high concentration of stress at the grain boundaries increases the dislocation density to a certain level, DRX occurs. Most of the recrystallized grains are located at the

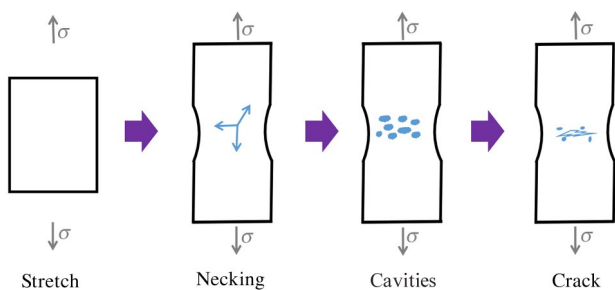


Fig.7 Schematic diagram of crack formation evolution

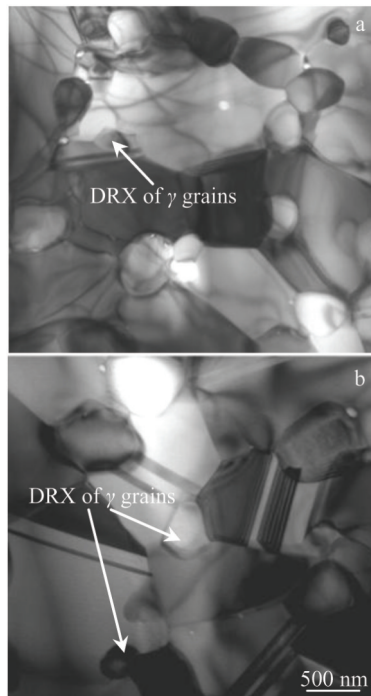


Fig.9 TEM images of DRX in Ti-45Al-7Nb alloy after tensile test at 1000 °C and strain rate of $5 \times 10^{-5} \text{ s}^{-1}$

grain boundaries, but a few of them are located near the dislocation edges and twins. DRX plays an important positive role in the plastic deformation of Ti-45Al-7Nb alloys, which is the stress relaxation mechanism for softening effect. DRX can also maintain the stable structure of the alloys, and lead to the even distribution of the microstructure and phase components of the alloys. Thus, the good mechanical properties of Ti-45Al-7Nb alloy can be obtained under the tensile conditions of temperature of 1000 °C and strain rate of $5 \times 10^{-5} \text{ s}^{-1}$.

3 Conclusions

1) The duplex Ti-45Al-7Nb alloys composed of γ -TiAl phase and α_2 -Ti₃Al phase are prepared by high-energy ball milling, vacuum hot pressing sintering, and hot extrusion methods.

2) As the temperature increases and the strain rate decreases, the tensile strength of Ti-45Al-7Nb alloys is decreased, while the elongation is gradually increased. The maximum elongation of alloy is 194% under the tensile condition of temperature of 1000 °C and strain rate of $5 \times 10^{-5} \text{ s}^{-1}$. The ultimate tensile strength of equiaxed fine-grained alloys is low, whereas the elongation is significantly increased due to the fine grains.

3) Ti-45Al-7Nb alloys produce a large number of cracks during high temperature plastic deformation, and the crack expansion direction is perpendicular to the tensile direction. The dislocations and twins are generated in the γ grains. The softening mechanism of the alloys is the dynamic recrystallization of the γ phase grains, which promotes the plastic deformation of alloys.

References

- Zhou H T, Kong F T, Wang X P et al. *Journal of Alloys and Compounds*[J], 2017, 695: 3495
- Chen G L, Xu X J, Teng Z K et al. *Intermetallics*[J], 2007, 15(5-6): 625
- Cheng L, Cheng H, Tang B et al. *Journal of Alloys and Compounds*[J], 2013, 552: 363
- Bewlay B P, Weimer M, Kelly T et al. *MRS Online Proceedings Library*[J], 2013, 1516: 49
- Chen G L, Zhang L C. *Mater Sci Eng A*[J], 2002, 329-331: 163
- Semiatin S L, Seetharaman V, Weiss I. *Mater Sci Eng A*[J], 1998, 243(1-2): 1
- Zhang W J, Francesconi L, Evangelista E. *Materials Letters*[J], 1996, 27(4-5): 135
- Chen Hua, Zhou Huimin, Zou Yang. *Rare Metal Materials and Engineering*[J], 2015, 44(10): 2387
- Wu G Q. *Materials Characterization*[J], 2004, 52(1): 81
- Sun H F, Li X W, Zhang P et al. *Materials Science and Engineering*[J], 2014, 611: 257
- Salishchev G A, Imayev R M, Senkov O N et al. *Mater Sci Eng A*[J], 2000, 286(2): 236
- Millett J C F, Jones B I P. *Materials & Design*[J], 1993, 14(1): 61
- Zhu Langping, Lu Xin, Hou Yaqing et al. *Rare Metal Materials and Engineering*[J], 2020, 49(10): 3460 (in Chinese)
- Liu He, Zhou Zhenhua, Liang Baoyan et al. *Powder Metallurgy Industry*[J], 2005, 15(3): 6 (in Chinese)
- Yu Hongbao, Chen Yuyong, Zhang Deliang et al. *Rare Metal Materials and Engineering*[J], 2008, 37(10): 1824 (in Chinese)
- Lin Peng, He Zhubin, Yuan Shijian et al. *Mater Sci Eng A*[J], 2012, 556: 617
- Liu Rutie, Li Xibin, Cheng Shihe. *Powder Metallurgy Industry* [J], 2001, 11(3): 51 (in Chinese)
- Yang Fan, Zhang Laiqi, Lin Junpin et al. *Intermetallics*[J], 2013, 33: 2
- Zhang W J, Chen G L, Appel F et al. *Mater Sci Eng A*[J], 2001, 315(1-2): 250
- Chen Guoliang, Sun Zuqing, Zhou Xing. *Mater Sci Eng A*[J], 1992, 153(1-2): 597
- Kothari K, Radhakrishnan R, Wereley N M. *Progress in Aerospace Sciences*[J], 2012, 55: 1
- Du Zhihao, Zhang Kaifeng, Jiang Shaosong et al. *Journal of Materials Engineering and Performance*[J], 2015, 24(10): 3746
- Liu Yong, Huang Boyun, He Yuehui et al. *The Chinese Journal of Nonferrous Metals*[J], 2000, 10(1): 59 (in Chinese)
- Liu Tingkun, Gao Yanfei, Bei Hongbin et al. *Journal of Materials Research*[J], 2018, 33(19): 3192
- Lin Peng, Tang Tingting, Chi Chengzhong et al. *Rare Metal Materials and Engineering*[J], 2018, 47(2): 416
- Liu Y, Liang X P, Liu B et al. *Intermetallics*[J], 2014, 55: 80
- Gerling R, Bartels A, Clemens H et al. *Intermetallics*[J], 2004,

- 12(3): 275
- 28 Zhang Chunping, Zhang Kaifeng. *Journal of Alloys and Compounds*[J], 2010, 492(1): 236
- 29 Wegmann G, Gerling R, Schimansky F P. *Acta Materialia*[J], 2003, 51(3): 741
- 30 Li Huizhong, Qi Yelong, Liang Xiaopeng et al. *Materials & Design*[J], 2016, 106: 90
- 31 Imayev V M, Imayev R M, Kuznetsov A V et al. *Mater Sci Eng A*[J], 2003, 348(1-2): 15

等轴细晶 Ti-45Al-7Nb 合金的高温机械性能及变形机制

王雪峥, 宋晓雷, 段振鑫, 陈 华

(长春工业大学, 吉林 长春 130012)

摘 要: 采用粉末冶金法制备了双相等轴细晶 Ti-45Al-7Nb (原子分数) 合金, 研究了该合金在温度为 900、950 和 1000 °C 以及应变速率为 1×10^{-3} 、 1×10^{-4} 和 $5 \times 10^{-5} \text{ s}^{-1}$ 条件下的高温力学性能, 并讨论了相应的变形机理。结果表明, 在高温或低应变率下, Ti-45Al-7Nb 合金的极限拉伸强度逐渐降低, 但伸长率显著增加。由于细小晶粒容易实现变形和协调, 其伸长率明显高于粗晶粒合金。高温拉伸后, 合金在裂缝处形成大量的空洞, 并在裂缝前部形成大量垂直于拉伸方向的长裂纹。此外, 晶界的滑动、晶粒的孪生和动态再结晶也导致了合金变形, 从而提高了微观组织的延展性。

关键词: 双相 TiAl 合金; 等轴细晶; 高温拉伸; 变形机理

作者简介: 王雪峥, 女, 1998 年生, 硕士生, 长春工业大学材料科学与工程学院, 吉林 长春 130000, E-mail: 1398894694@qq.com